REPORT DOCUMENTATION PAGE

Form Approved OMB No. 0704-0188

1. AGENCY USE ONLY *(Leave blank)*	2. REPORT DATE	3. REPORT TYPE AND DATES COVERED
	December 1992	Proceedings, 1991 to 1992

4. TITLE AND SUBTITLE Acoustical Scattering From Atmospheric Turbulence

5. FUNDING NUMBERS

DA PR: N/A
PE: N/A

6. AUTHOR(S) Harry J. Auvermann (ARL), George H. Goedecke (New Mexico State University)

7. PERFORMING ORGANIZATION NAME(S) AND ADDRESS(ES)
U.S. Army Research Laboratory
Attn: AMSRL-IS-EP email: hauvermann@arl.mil
2800 Powder Mill Road
Adelphi, MD 20783-1197

8. PERFORMING ORGANIZATION REPORT NUMBER

9. SPONSORING/MONITORING AGENCY NAME(S) AND ADDRESS(ES)
U.S. Army Research Laboratory
White Sands Missile Range, NM 88002-5501

10. SPONSORING/MONITORING AGENCY REPORT NUMBER

11. SUPPLEMENTARY NOTES
ARL PR: N/A
AMS code: N/A

Published in Proceedings of the 1992 Battlefield Atmospherics Conference, Fort Bliss, TX, 1–3 December 1992, pp 43–52

12a. DISTRIBUTION/AVAILABILITY STATEMENT
Approved for public release; distribution unlimited.

12b. DISTRIBUTION CODE

13. ABSTRACT *(Maximum 200 words)*

The objective of the ASL research effort in acoustic propagation is to provide the Army with a multi-stream model for investigating acoustic detection systems. The first step in developing this model is to account for turbulent scattering. Five elements are necessary to accomplish this step—(1) model the turbulent region as a collection of vortices with a distribution of characteristic sizes/velocities; (2) characterize each vortex (turbule) as a known (or assumed) velocity distribution in three space; (3) solve the fluid equations to determine the scattering from each turbule; (4) sum the contributions to the scattered sound pressure level at the detector location of all turbules accounting for the propagation characteristics of the atmospheric medium; and (5) incorporate the algorithms devised above into existing (or appropriately modified) propagation models. Progress in these five areas will be reported.

14. SUBJECT TERMS
Turbulence model, turbule scattering, acoustic propagation

15. NUMBER OF PAGES
14

16. PRICE CODE

17. SECURITY CLASSIFICATION OF REPORT	18. SECURITY CLASSIFICATION OF THIS PAGE	19. SECURITY CLASSIFICATION OF ABSTRACT	20. LIMITATION OF ABSTRACT
Unclassified	Unclassified	Unclassified	SAR

PROCEEDINGS
of the

1992 Battlefield Atmospherics Conference

Fort Bliss, Texas
1-3 December 1992

BATTLEFIELD ENVIRONMENT DIRECTORATE
U.S. Army Research Laboratory
White Sands Missile Range
New Mexico

PROCEEDINGS

of the

1992 BATTLEFIELD ATMOSPHERICS CONFERENCE

1–3 December 1992

Sponsor

Battlefield Environment Directorate
U.S. Army Research Laboratory
White Sands Missile Range, New Mexico

Conference Manager

Mr. Robert Lee
U.S. Army Research Laboratory

Conference Chairman

Mr. Edward Creegan
U.S. Army Research Laboratory

Host

Fort Bliss, El Paso Texas

CONTENTS

ACOUSTICAL SCATTERING FROM ATMOSPHERIC TURBULENCE

Harry J. Auvermann
Battlefield Environment Directorate*
White Sands Missile Range, New Mexico 88002-5501, USA

George H. Goedecke
New Mexico State University
Las Cruces, New Mexico 88003, USA

ABSTRACT

The objective of the ASL research effort in acoustic propagation is to provide the Army with a multi-stream model for investigating acoustic detection systems. The first step in developing this model is to account for turbulent scattering. Five elements are necessary to accomplish this step--(1) model the turbulent region as a collection of vortices with a distribution of characteristic sizes/velocities; (2) characterize each vortex (turbule) as a known (or assumed) velocity distribution in three space; (3) solve the fluid equations to determine the scattering from each turbule; (4) sum the contributions to the scattered sound pressure level at the detector location of all turbules accounting for the propagation characteristics of the atmospheric medium; and (5) incorporate the algorithms devised above into existing (or appropriately modified) propagation models. Progress in these five areas will be reported.

1. INTRODUCTION

Acoustic propagation in the atmosphere is influenced by a number of factors that have to be considered in any model designed to predict detector response at battlefield distances. Figure 1 illustrates a possible scenario that, along with fig. 2, incorporates most of the factors of interest. Figure 1 shows an object of interest marked S that is a source of the acoustic field marked F. An acoustic detector marked D is some distance from the source. An obstruction marked O illustrated as a ridge intervenes between S and D. Atmospheric turbulence is marked T and the reflecting ground surface is marked P. E, M, and R are the diffracted, turbulence scattered, and reflected fields, respectively. The electronic signal from D marked V is produced by a superposition of the direct field F (if any) with E, M, and R plus the intrinsic detector noise denoted by N. The problem of interest is to determine theoretically the total field given the scenario. The importance of acoustics as a non-line-of-sight detection tool for the Army is also illustrated in fig. 1. The detector is shown in what is known as a shadow zone by analogy with ray propagation from optics.

A shadow zone can also be produced by an upwardly refracting atmosphere. This effect is illustrated in fig. 2. In the figure, a source is located at an elevation of 10 m in an atmosphere with a constant sound speed gradient. The ray

*formerly U.S. Army Atmospheric Sciences Laboratory (ASL)

path shown just grazes the ground and is known as the limit ray. The shadowzone is to the right of the curve minimum and between the curve and the range axis. The indicated height at a range of 7000 m is 174.89 m. The shadow zone begins at a range of 1351.32 m. Current acoustic propagation models do not account for terrain induced shadow zones as depicted in fig. 1 but are able to model propagation in a stratified atmosphere whose characteristics vary only with height as that depicted in fig. 2.

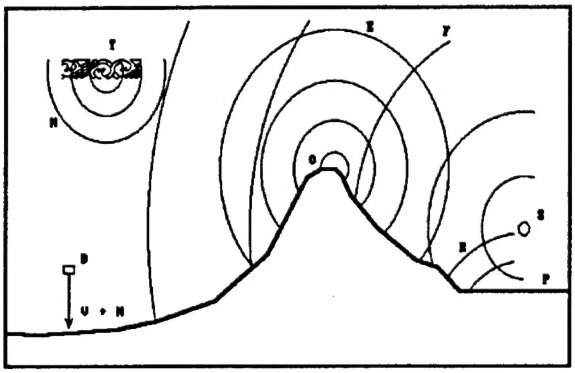

Figure 1. Acoustic detection scenario.

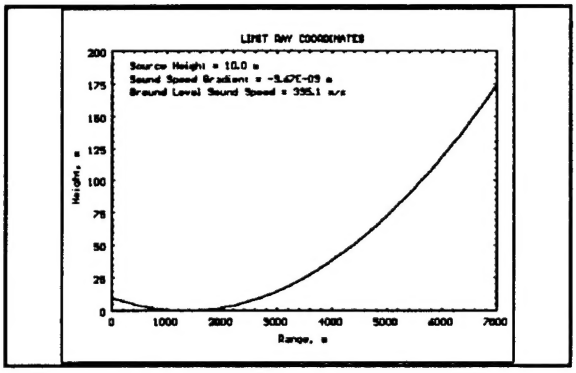

Figure 2. Limit ray coordinates locating the shadow zone.

2. WAVE SOLUTIONS FOR ACOUSTIC FIELDS

While the ray solution shown in fig. 2 accounts for the constant atmospheric sound speed gradient, it does not account for the reflections that occur at the ground nor does it account for the wave nature of sound. Figures 3 and 4 illustrate the effect of the ground but not the full-wave nature of sound. As a check on the more sophisticated models, a propagation model called here SPHERICAL was written that models a uniform atmosphere situated above a flat earth, the latter modeled by an impedance change. These plots using data produced by SPHERICAL are essentially ray solutions with the ground effect modeled as an image source below ground level, with the image field phase and amplitude modified according to the impedance discontinuity. Figure 3 shows a contour plot from SPHERICAL that represents the sound field for a uniform atmosphere, frequency of 170 hertz, source height of 10.0 m, sound speed 335.1 m/s, and a ground impedance ratio of 8.44 + j10.0. The heavy line is the limit ray position from fig. 2. Figure 4 shows the region near the origin in greater detail with the horizontal and vertical scales the same. Interference between the direct and the ground reflected waves is clearly demonstrated.

To demonstrate the full-wave nature of sound propagation, a more sophisticated model is necessary. The fast field program (FFP) (Raspet, 1985) is a full-wave solution to the propagation equation that accounts for a nonuniform atmosphere using horizontal planar layers, the propagation constants of each layer being uniform. Ground effects are introduced by an impedance boundary just as in the SPHERICAL program. Since the ultimate goal was to model turbulence effects as scattering, FFP was included as a subroutine in a driver that produced data from multiple sources, multiple scatterers, and multiple detectors. This program is named the acoustical multistream propagation program (AMPP) (Auvermann, 1992). AMPP loops through a set of sources, a set of scatterers, and a set of detector positions, saving the sound field results of each calculation. The

results for the detector position set provides the data for contour plots shown below. AMPP preserves the sound pressure amplitude and phase, as well as the exitance (watts/square meter) so that a coherent summation is possible for a reasonable number of sources or scatterers. This coherent summation capability of AMPP has not been exercised because of the diversion caused by the interesting feature of the field in shadow zones that is discussed below.

To exercise the AMPP program, the scenario of fig. 1 was calculated for an upward refracting atmosphere. The results are shown in figs. 5 and 6. The uniform sound speed gradient was $-3.67 \cdot 10^{-3}\ s^{-1}$, with speed at zero height of 335.1 m/s and a ground impedance ratio as in the SPHERICAL program results of figs. 3 and 4. The heavy line in each figure is the limit ray path from figure 2. As seen by comparison of fig. 5 with fig. 3, SPHERICAL and AMPP show virtually identical contours out to a range of 1000 m. Beyond 1000 m, the AMPP upper contour parallels the limit ray path to a high degree of accuracy. The plot in fig. 6 shows in greater detail the sound exitance level in the shadow zone below the limit ray path for the range interval 5000 m to 7000 m.

Finding unexpectedly high sound levels in the shadow zone has diverted the investigation of turbulence scattering into this region because the expected scattered level was approximately the same. The nature of the nonturbulence related sound level was investigated. To eliminate the possibility that computational precision was inadequate, AMPP was changed to 64-bit precision. The code was run at higher frequencies, which should produce faster roll-off at the shadow zone boundary. Changes of ground impedance by an order of magnitude in either direction and a three-to-one increase of sound speed gradient were tried. All these changes produced no material change in the results. The conclusion was that the sound levels reported by AMPP are real and to be expected. The mechanism is most likely the reflection of a spherical wave by a plane boundary, which will produce a field somewhat more complicated than that of the reflection of a plane wave at a plane boundary. To expedite the turbulence investigation, an artificially attenuated shadow zone contour picture was constructed as reported in section 5.

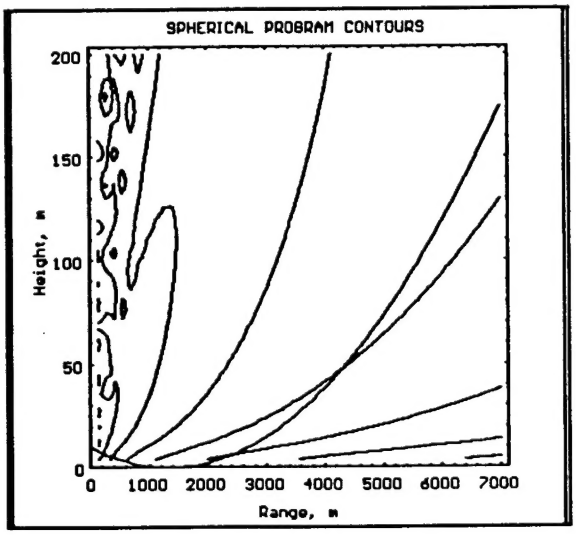

Figure 3. Uniform atmosphere contours.

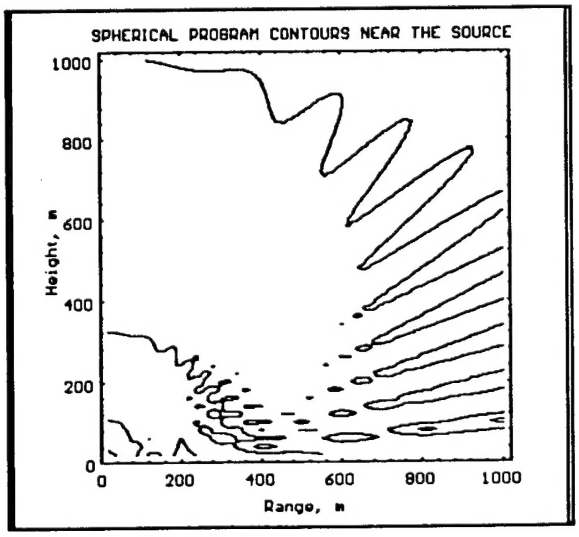

Figure 4. SPHERICAL program contours near the source.

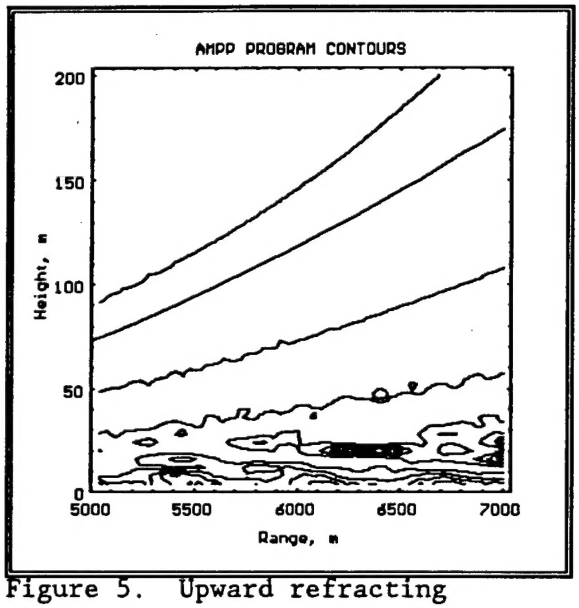

Figure 5. Upward refracting atmosphere results.

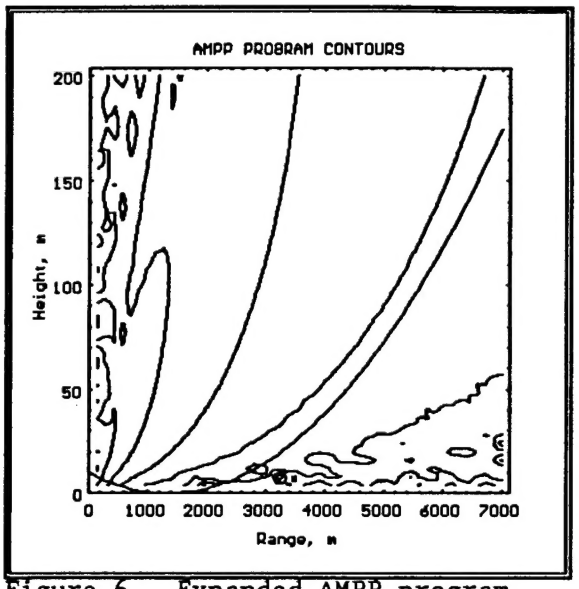

Figure 6. Expanded AMPP program results for longer ranges.

3. SCATTERING BY TURBULENCE

Following the "structural approach" to turbulence, acoustical scattering from turbulence is by analogy with optical scattering from aerosols considered as scattering from a collection of eddies (or turbules as hereinafter referred to) of different sizes with a number concentration assigned to each size. If the scattering cross section and number concentration for each size class is available, then a scattering calculation can be made using the geometry of fig. 7. Figure 7 shows a source, a detector, and a turbule positioned over flat ground. The coordinate system to be used is also shown. The horizontal coordinate variable is r and the vertical coordinate variable is z. The scattering angle variable θ is also shown. The quantities R_{st}, R_{td}, and R_{sd} are slant ranges. In this paper, all distances are expressed in meters. The coordinates of the principal objects chosen for this scenario and the associated slant ranges are as follows:

$r_s = 0.0, \quad z_s = 10.0 \qquad R_{st} = 5{,}053.588$
$r_t = 5000.0, \quad z_t = 744.0 \qquad R_{td} = 1{,}246.409$
$r_d = 6000.0, \quad z_d = 0.0 \qquad R_{sd} = 6{,}000.008$

Subscripts s, t, and d stand for source, turbule, and detector, respectively. With this geometric arrangement the scattering angle is $\theta = \pi/4$ radians. Symbols to be used and not already defined are listed in table 1 along with units and values.

The value of Ω_d in table 1 was chosen as representative, leading to the determination of the scattering volume from eq. (1).

$$\Omega_d = 2\pi[1 - \cos(\phi)] \qquad r_v = R_{td} \sin(\phi) \qquad V_{sca} = \pi\, r_v^2\, l \tag{1}$$

Assuming an isotropic source in an infinite, lossless uniform medium, the exitances at the turbule and at the detector are

$E_{It} = E_s\,(R_s/R_{st})^2 = 3.9156 \cdot 10^{-8}$ $\quad L_{It} = 10\,\log_{10}(E_{It}/E_s) = -74.07$ dB

$E_{Id} = E_s\,(R_s/R_{sd})^2 = 2.7777 \cdot 10^{-8}$ $\quad L_{Id} = 10\,\log_{10}(E_{Id}/E_s) = -75.56$ dB

The logarithmic equivalent of these quantities, called level and expressed in decibels (dB), is given above also. The letter I in the subscripts indicates these quantities are infinite space values. In table 1, E_t was set equal to E_{It}. Equation (2) is used to calculate the scattered exitance.

$$\sigma_{sca}(a,v,\theta) = \pi a^2 \langle Q^{(1)}(k,\hat{r}) \rangle \qquad \sigma_{sca}(v,\theta) = \int_0 da\, \sigma_{sca}(a,v,\theta)\, n_a(a)$$

$$E_d = \frac{E_t \sigma_{sca}(v,\theta)\, V_{sca}}{R_{td}^2} \tag{2}$$

The nature of the turbule concentration function $n_a(a)$ in eq. (2) is not known at this time so an approximate evaluation of the integral over turbule size will be made. This approximation will involve selection of a typical size a_t and a corresponding typical number concentration n_t with the integral being given by the product of n_t and $\sigma_{sca}(a_t,v_t,\theta)$, where v_t is the velocity of the typical turbule. The scattering volume V_{sca} is that of a length 1 cylinder with a radius at midpoint set by the detector field of view Ω_d.

The scattering efficiency of turbules was determined previously (Goedecke, 1992). Theory was developed for acoustical scattering by localized quasi-static atmospheric turbules that contain both flow and sound speed variations. Differential and total cross-section expressions have been found for a Gaussian spinning turbule model of effective radius $\underline{a}$ by using the first Born approximation, which is estimated to be valid for $ka < 5$ for $v_{max}/c_\infty < 0.1$. The contributions of the sound speed variation are about three orders of magnitude smaller than those of the flow. The latter are proportional to $(ka)^6$ and $[\sin(\theta)\,\cos(\theta)\,\cos(\theta_\alpha)\,\sin(\phi - \phi_\alpha)]^2$, where (θ,ϕ) are the (polar, azimuthal) scattering angles, $(\theta_\alpha,\phi_\alpha)$ are the spin axis angles. The contributions of the sound speed inhomogeneities vary as $(ka)^4$ and have a somewhat Rayleigh-like dependence on θ.

Analytical results from this theory for turbule scattering efficiency averaged over turbule spin axis orientation are used above. These results are summarized here. A model spinning turbule was chosen to have the following (quasi) static flow velocity $\vec{v}(\vec{r})$:

$$\vec{v}(\vec{r}) = (\vec{\Omega} \times \vec{r}) \exp(-r^2/a^2) \qquad \Omega = (2e)^{1/2} v_t/a\,. \tag{3}$$

This equation represents a nonuniformly spinning turbule, with angular velocity parameter Ω about an axis $\hat{\Omega}$ through the origin of coordinates. The quantity c_∞ is the background wave speed far from the turbule; the parameter $\underline{a}$ is an "effective radius" of the turbule; and $\vec{r}$ is the position vector. The expression for Ω relates the angular velocity to the maximum turbule velocity which occurs at $r = a/2^{1/2}$.

If an acoustic plane wave with propagation vector $\vec{k}$, where $k = 2\pi/\lambda$, is incident upon this model turbule, then the first order in Ω differential scattering

efficiency, which is defined to be the scattering cross section divided by the physical cross-section πa^2, averaged over all spin axis orientations is

$$\langle Q^{(1)}(k,\hat{f})\rangle = \left(\frac{1}{3}\right)\left(\frac{\Omega a}{4c_\infty}\right)^2 (ka)^6 (\sin\theta\cos\theta)^2 \exp[-(ka)^2(1-\cos\theta)] \quad . \quad (4)$$

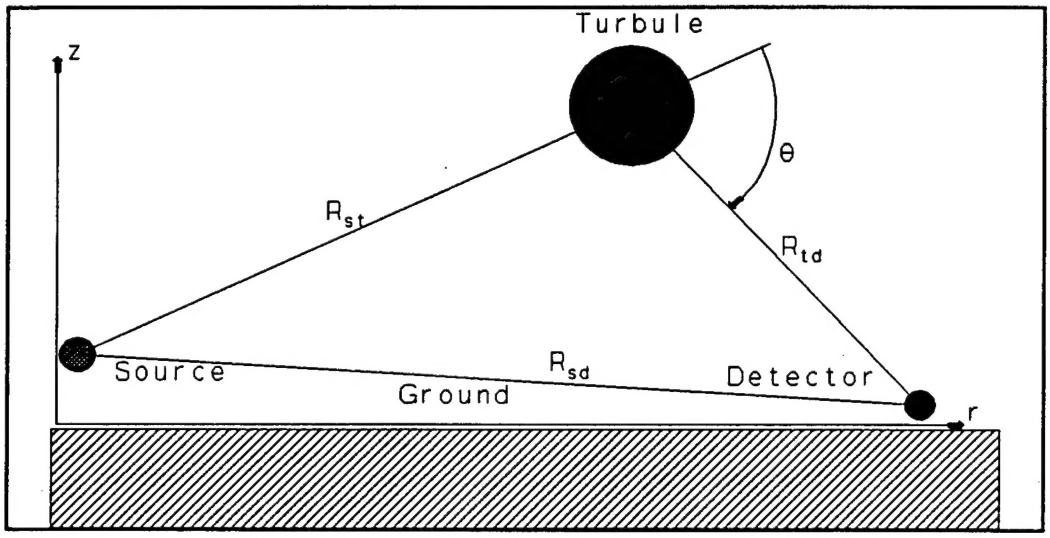

Figure 7. Turbulence scattering geometry.

TABLE 1. SYMBOL DEFINITIONS

Symbol	Definition	Value	Units
a	turbule characteristic size		m
a_t	typical turbule size	$17.5/\pi$	m
v	turbule characteristic velocity		$m \cdot s^{-1}$
v_t	typical turbule maximum velocity	1.340	$m \cdot s^{-1}$
Ω	turbule angular velocity	0.561	$rad \cdot s^{-1}$
λ	acoustic wavelength	10.0	m
θ	propagation to detector angle	$\pi/4$	radian
$\langle Q^{(1)}(k,\hat{f})\rangle$	differential scattering efficiency	$5.52 \cdot 10^{-5}$	
$\sigma_{sca}(a,v,\theta)$	differential scattering cross section	$1.49 \cdot 10^{-3}$	m^2
R_s	reference distance from source	1.0	m
E_s	exitance of source at R_s	1.0	$w \cdot m^{-2}$
E_t	exitance at scattering volume	$3.92 \cdot 10^{-8}$	$w \cdot m^{-2}$
E_d	scattered exitance at detector	$9.99 \cdot 10^{-12}$	$w \cdot m^{-2}$
Ω_d	detector solid angle field	1.0	str.
$n_a(a)$	turbule concentration distribution		m^{-3}
n_t	typical turbule concentration	$(1/17.5)^3$	m^{-3}
l	length of scattering volume	1000.0	m
r_v	radius of scattering volume	674.6	m
ϕ	detector field half-angle	0.572	radian
V_{sca}	scattering volume	$1.43 \cdot 10^9$	m^3

Figures 8 and 9 show the turbule scattering properties to first order in $\Omega a/c_\infty$.

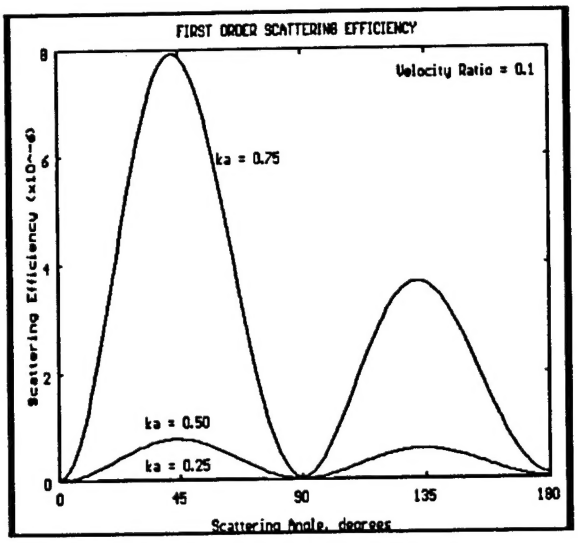

Figure 8. Average differential scattering efficiency.

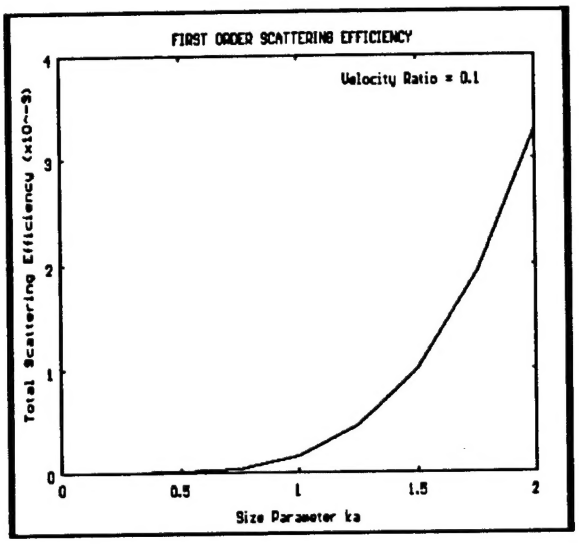

Figure 9. Total average scattering for a spinning turbule.

The typical value for turbule size was chosen from the size parameter for which the cross section is near maximum. Solving for a_t gives the value in table 1.

$$2\pi\ a_t/\lambda = 3.5 \tag{5}$$

Since the diameter of the turbule is approximately $35/\pi$, a cell size is chosen to be 17.5 or slightly larger than the turbule. The cell is thought of as a cube that completely contains one turbule. The number concentration will be the reciprocal of the cell volume, which is the value for n_t given in table 1. The final parameter to be determined is the typical turbule velocity. To make a reasonable choice of v_t, it is appropriate to choose an outer scale size related to the dimensions of the scattering volume and to choose the velocity of the maximum sized turbule as a reasonable wind speed. Thus, if the maximum turbule size is considered to be 500.0 m and the wind speed is 6.0 m • s^{-1}, the one-third power law of velocities determines the typical maximum velocity from the relation

$$v_t = 6.0\ (a_t/500.0)^{1/3}\ , \tag{6}$$

again giving the value in table 1. The differential scattering efficiency is determined by using eq. (4); the turbule scattering cross section, the scattering cross section per unit volume, and the scattered exitance at the detector are determined by using eq. (2).

4. COMPARISON OF RESULTS

The purpose of this section is to compare the scattered exitance derived in section 3 with that calculated from the "statistical approach" relations as well as with experimental results (Gilbert, 1990). The standard statistical approach scattering cross section is (Tatarskii, 1971)

$$\sigma_{Tat}(\theta) = 0.38 k^{1/3} \left[\frac{(\cos(\theta))^2}{(2\sin(\theta/2))^{11/3}} \right] \left[\frac{C_v^2}{c_\infty^2} (\cos(\theta/2))^2 + 0.13 \frac{C_T^2}{T_\infty^2} \right] . \quad (7)$$

The symbols that have not been defined before are C_v^2, the velocity structure constant, C_T^2, the temperature structure constant, and T_∞, the ambient temperature. Equation (7) has been rederived with fewer approximations but the result has not been reported. The derivation is too lengthy to include here, but the final result is

$$\sigma_{sta}(\theta) = 2\pi k^4 \left[\frac{B^v(k)}{c_\infty^2} (\cos(\theta) \cos(\theta/2))^2 + \frac{B^T(k)}{4 T_\infty^2} \right]$$

$$B^v(k) = 4.16 C_v^2 \qquad B^T(k) = 4.16 C_T^2 \quad (8)$$

$$C_v^2 = 0.04 \ (m \cdot s^{-1})^2 m^{-2/3} \qquad C_T^2 = 0.00043 \ k^2 m^{-2/3} .$$

The numerical constant 4.16 (dimensions of $m^{11/3}$) in the expressions for $B^v(k)$ and $B^T(k)$ in eq. (8) follows approximately the angle dependence of the first bracket in eq. (7) and has been determined for an angle of $\pi/4$ radians. The structure constants were taken from the literature of Brown (1976). When an asymptotic wave speed of 335.1, a temperature of 300 k, and eqs. (7) and (8) are used, the statistical and Tatarskii cross sections are

$$\sigma_{sta}(\theta) = 6.2417 \cdot 10^{-7} \ m^{-1} \qquad \sigma_{Tat}(\theta) = 1.3217 \cdot 10^{-7} \ m^{-1} . \quad (9)$$

Detected exitance using eq. (2) and excess loss levels for the four cases of interest are brought together in table 2.

TABLE 2. DETECTED FIELDS COMPARISON

Symbol	Definition	Value	Units
E_d	exitance, structural approach	$9.99 \cdot 10^{-12}$	$w \cdot m^{-2}$
E_{sta}	exitance, statistical approach	$2.25 \cdot 10^{-11}$	$w \cdot m^{-2}$
E_{Tat}	exitance, Tatarskii formula	$4.76 \cdot 10^{-12}$	$w \cdot m^{-2}$
L_d	excess loss, structural approach	34.44	dB
L_{sta}	excess loss, statistical approach	30.91	dB
L_{Tat}	excess loss, Tatarskii formula	37.66	dB
L_{lit}	excess loss, literature value	20 - 30	dB

A number of issues impact the validity of the excess loss values in table 2. L_d was calculated using an assumed turbule number concentration and velocity and a typical turbule size rather than an integration over a size distribution. L_{sta} was calculated using eq. (8), which was derived using a realistic structure function that became constant at large seperations. Perhaps this is the reason for the difference between L_{sta} and L_{Tat}. L_d and L_{sta} are near the spread in L_{lit}. The latter, however, was measured for a different geometry and different frequency. The fact that the new results, as crude as represented here, give answers in general agreement with the statistical approach and with the experiment is encouraging.

5. TURBULENT SCATTERING IN A PROPAGATION MODEL

Figures 10 through 12 show inclusion of turbulent scattering in a propagation model by running AMPP twice and summing the results. The first run preserves the field produced by the source (fig. 10). Figure 10 is a reproduction of figure 6 except the shadow zone has been artificially cleared of residual sound levels. The second run preserves the field produced by an isotropic scatterer, the results being shown in fig. 11. The two results are combined after the second run results have been modified by the source to turbule loss. This final result is shown in fig. 12 where the summation has been done incoherently. Figure 12 only gives a representative picture of the superimposed fields because the solution algorithm of AMPP (from FFP) can only model isotropic scatterers; whereas, it is known that scatterers have patterns resembling fig. 8. The scattered exitance in fig. 12 has been adjusted to give an excess loss at the detector location of fig. 7 of approximately 25 dB.

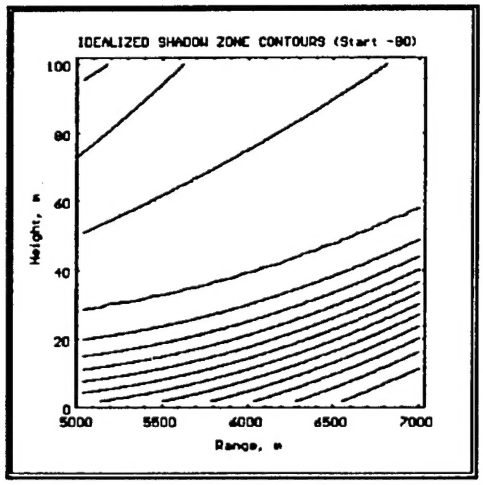

Figure 10. Idealized shadow zone zone contours (contours at -80 to -145).

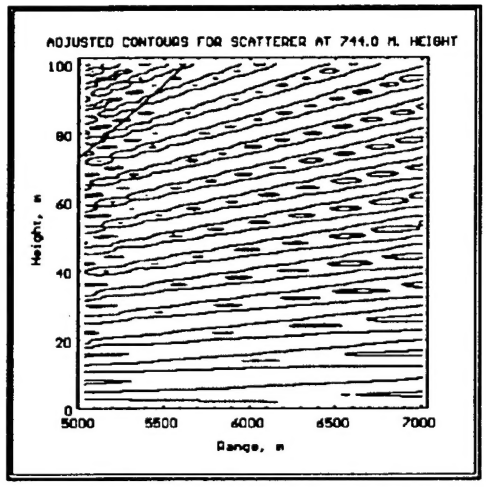

Figure 11. Adjusted scattered field (contours at -100, -105, and -110).

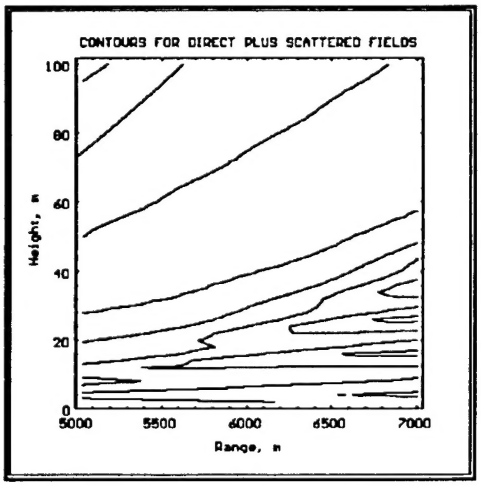

Figure 12. Combined primary and scattered fields (contours at -80 to -110 in 5 dB intervals).

6. CONCLUSIONS

The "structural approach" to modeling turbulence produces scattered sound levels that are in general accordance with those calculated using the "statistical approach." They are also in accordance with the experiment. The claim is not that a turbulent region is made up only of a collection of turbules of various sizes. Rather, the claim is that such a concept is a first approximation to the true distribution of motion, energy, and density in the turbulent region. Furthermore, as far as scattering is concerned, this concept yields reasonable answers. The significance of the work reported here is that a pathway has been charted that breaks the shackles imposed by the isotropic and homogeneous requirements of the statistical approach. Boundary layer theory and the vertical structure capability of current acoustic propagation models both attest to the recognized fact that the atmosphere is not isotropic and homogeneous. The structural approach supported by analytical or numerical knowledge of the scattering properties of turbules does work. What has not been done yet is to determine the number concentration distribution appropriate for use. Additionally, knowledge of the scattering properties of large turbules is yet to be determined. The true internal structure of a turbule has not been determined, but the scattering results do not seem to be very sensitive to this structure. Use of the structural approach requires that the analyst know something more of the details of the turbulent region than the statistical approach. A simulation of flow in the actual environment being analyzed is indicated. Calculation of scattering from such unusual features as intermittent turbulent regions is possible. It will be necessary to devise a method by which anisotropic sources and scatters can be included in propagation models.

REFERENCES

Auvermann, H. J., R. L. Reynolds, and D. M. Brown, 1992: Development of a Multistream Acoustic Propagation Model Including Turbulent Scattering. Technical Report (Draft), U. S. Army Atmospheric Sciences Laboratory, White Sands Missile Range, NM 88002.

Brown E. H., and S. F. Clifford, 1976: On the attenuation of sound by turbulence. J. Acoust. Soc. Am. 60(4).

Gilbert, K. E., R. Raspet, and Xiao Di, 1990: Calculation of turbulence effects in an upward-refracting atmosphere. J. Acoust. Soc. Am. 87(6).

Goedecke, G. H., 1992: Scattering of Acoustical Waves by a Spinning Atmospheric Turbule. Contractor Report (Draft), U. S. Army Atmospheric Sciences Laboratory, White Sands Missile Range, NM 88002.

Raspet, R., S. W. Lee, E. Kuester, D. C. Chang, W. F. Richards, R. Gilbert, and N. Bong, 1985: A fast-field program for sound propagation in a layered atmosphere above an impedance ground. J. Acoust. Soc. Am., 77(2).

Tatarskii, V. I., 1971, The Effects of the Turbulent Atmosphere on Wave Propagation. TT-68-50464, National Technical Information Service, Springfield, VA 22161.